# Changes in Resistivity and Composition of Chemical Vapor Deposited Tungsten Silicide Films by Annealing

**Yoshimi Shioya, Takahiro Itoh, Ikuro Kobayashi, and Mamoru Maeda**

*Fujitsu Limited, Process Development Department, 1015 Kamikodanaka, Nakahara-ku, Kawasaki 211, Japan*

## ABSTRACT

Chemical vapor deposited (CVD) tungsten silicide films were formed by a cold wall reactor. These films were annealed in $N_2$ to investigate changes in resistivity, composition, thickness, and impurity. The change in resistivity after 1000°C annealing becomes larger as the film reaches the stoichiometric value. A composition change occurs in a film whose composition Si/W is more than 2.6. Excess Si in the $WSi_x$ films ($x > 2.6$) is segregated in the boundary between $WSi_x$ and poly-Si. A thickness change of about 15% occurs after 1000°C annealing at $WSi_{2.4}$ on $SiO_2$; this value is smaller than the calculated value. F and H, which are impurities in $WSi_x$ films decrease gradually and diffuse into gate $SiO_2$ after 1000°C annealing.

Progress of metal oxide semiconductor (MOS) large scale integrated circuits (LSI) is remarkably fast. Since the one kilo bit dynamic random access memory (1 Kbit DRAM) was developed in 1970, integration has advanced 4 times every 3 years. Now, one mega bit (1 Mbit) DRAM has been manufactured as a trial. The design rule for 1 Mbit DRAM is 1.2-1.3 μm, and the cell area has become very small: ranging from 20 to 35 $\mu m^2$. For this reason, new capacitor structures such as trench and stacked capacitors are used (1-4). $TiSi_2$, $TaSi_2$, and other refractory metal silicides with a base layer of poly-Si and refractory metals such as W are being used as interconnection materials.

The reason for employing refractory metals or refractory metal silicides is that as the linewidth becomes narrower and line length longer, resulting in high densification of devices, the signal propagation delay times become larger with the usually used poly-Si interconnection. Currently, there are two methods for forming these films: the physical vapor deposition (PVD) method, and the chemical vapor deposition (CVD) method.

Among these methods, the CVD method is frequently used because of good step coverage. For example, we refer to the studies on deposition of $WSi_2$ films by plasma CVD (5, 6). The low pressure chemical vapor deposited $WSi_x$ film, developed by Brors *et al.*, however, is beginning to be widely used because of lower contamination and resistivity (7). Detailed reports on resistivity and capacitance-voltage characteristics have already been written.

Generally, electrical characteristics degrade in the reaction between poly-Si and $SiO_2$ during high temperature annealing (8). Consequently, it is necessary to study reactions and composition changes which include changes of F and H in the $WSi_x$ film by annealing; the mechanism of change also needs to be studied. Hara, *et al.* reported that reaction between $WSi_x$ film and the reaction between poly-Si and $SiO_2$ begins at 1000°C (9).

We report on the changes in resistivity, composition, and behavior of F and H as well as the decreasing film thickness after annealing.

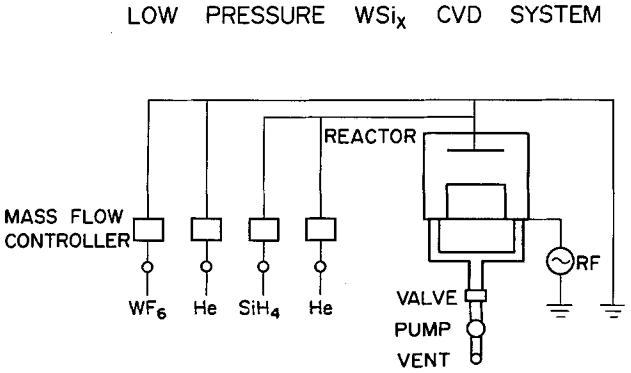

Fig. 1. Schematic diagram of the cold wall CVD equipment

## Experimental

$WSi_x$ films were formed by cold wall CVD (see Fig. 1). $WF_6$ and $SiH_4$ were used as reaction gases. The flow rate of $WF_6$ was fixed to 2 cm³/min, but the flow rate of $SiH_4$ was varied from 30 to 120 cm³/min. Helium was used as a dilution gas. The substrate temperature was changed from 325° to 425°C. The pressure was 40 Pa. The $WSi_x$ films were deposited on the (100) plane, the poly-Si plane, and the oxidized plane of a 4 in. Si wafer. Film composition was controlled by changing the substrate temperature. Samples were annealed for 30 min in $N_2$, therefore preventing $O_2$ contamination. Film thickness was measured by Talystep after etching with $HNO_3$:HF (ratio was 50:2). The resistivity was measured by a 4 point probe. Film composition was analyzed by Rutherford backscattering (RBS) method. The energy of the He ion was 2.275 MeV. The annealing behavior of impurities in these films was analyzed by secondary ion mass spectrometry (SIMS).

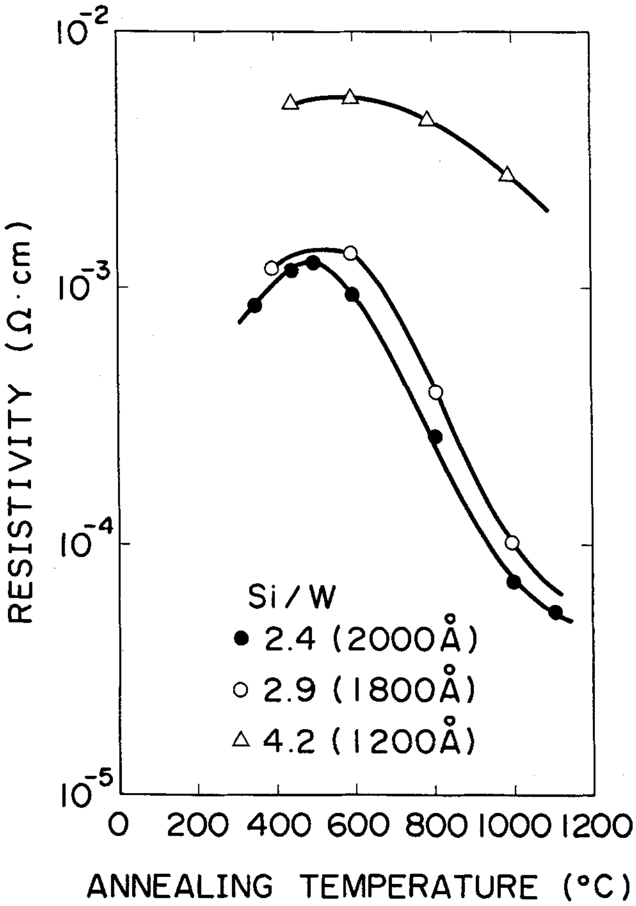

Fig. 2. Annealing temperature effect on resistivity for three different compositions.

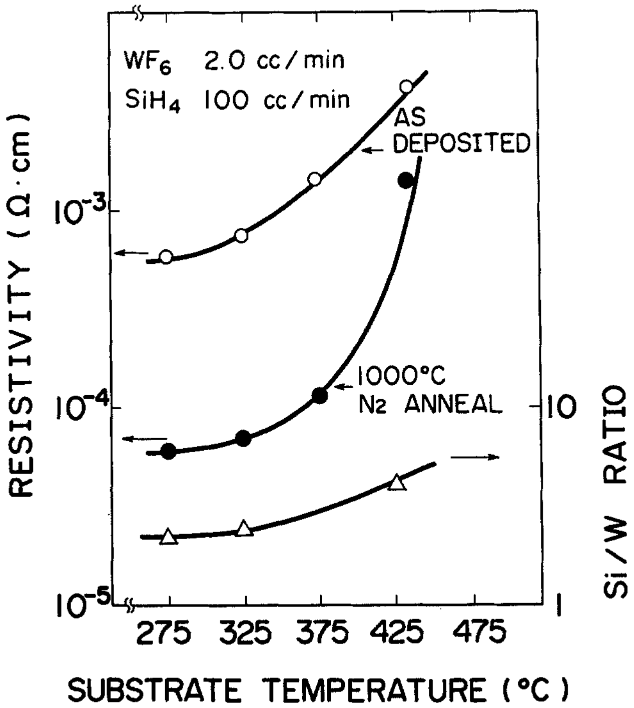

**Fig. 3.** Change in resistivity between as-deposited state and after 1000°C annealing.

## Results and Discussion

*Change in resistivity of WSi$_x$ film after annealing.*—The resistivity as a function of annealing temperature for three different compositions is shown in Fig. 2. Film thicknesses range from 1200 to 2000Å. The resistivity after 1000°C annealing decreases by about one order of magnitude over the as-deposited state. The resistivity reaches a maximum between 500° and 600°C. This maximum is considered to be caused by the crystallization of WSi$_x$ that has a predominately hexagonal structure (10).

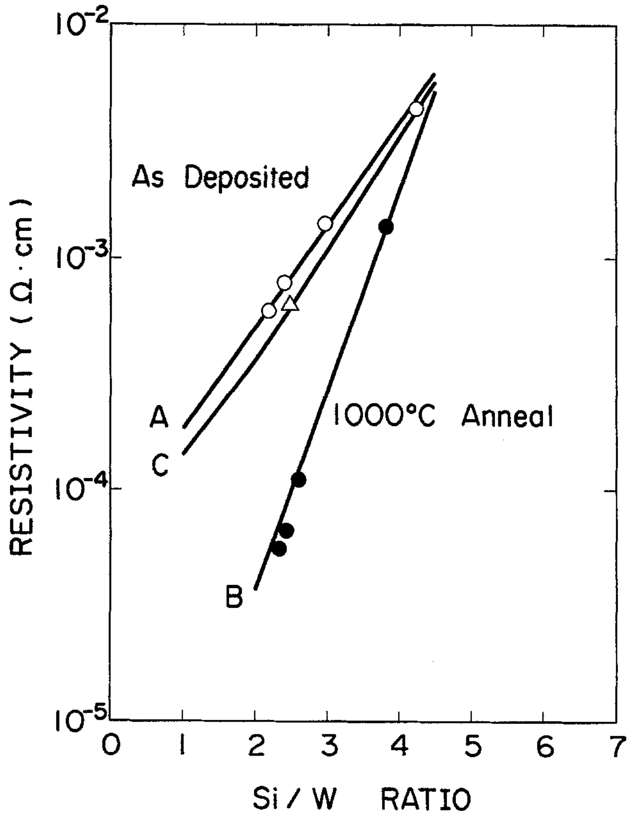

**Fig. 4.** Effect of composition on change in resistivity. A is the resistivity in the as-deposited state, B is the resistivity after 1000°C annealing, and C is the resistivity calculated by decreasing of the film thickness only. Δ is calculated value from the measured decrease of WSi$_x$ film thickness.

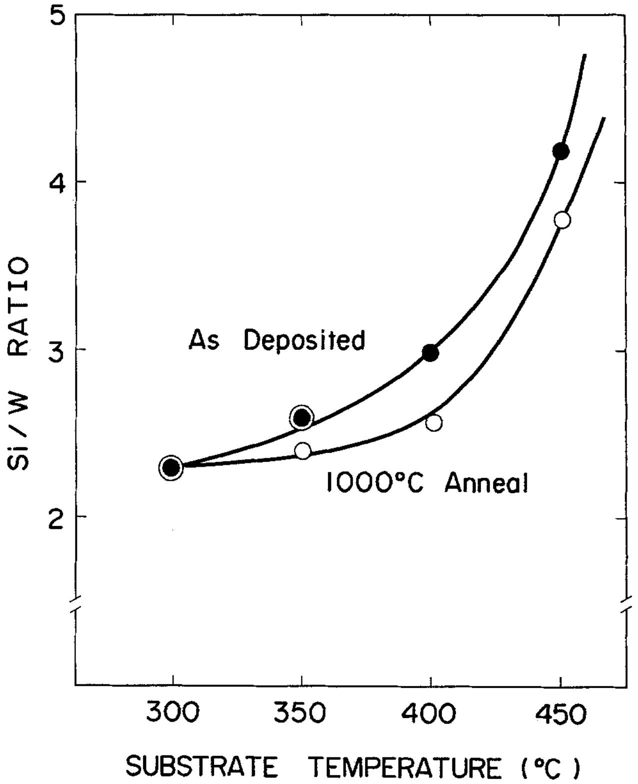

**Fig. 5.** Change in composition before and after 1000°C annealing as a function of substrate temperature.

Changes in resistivity between the as-deposited state and after 1000°C annealing for several substrate temperatures are shown in Fig. 3. It was observed that the ratio of change in resistivity that is represented as $(\rho_{\text{as-deposited}}-\rho_{1000^{\circ}\text{C annealed}})/\rho_{\text{as-deposited}}$ becomes larger as the substrate temperature decreases. To investigate this phenomenon in more detail, the relation of composition to resistivity is represented graphically in Fig. 4. In other words, the ratio of change in resistivity becomes larger as the Si/W ratio becomes smaller. From this figure, logarithmical resistivities before and after 1000°C annealing are found to have a linear relation to the composition as expressed in Eq. [1] and [2]

$$\log \rho_{\text{as-deposited}} = K_1\,(\text{Si/W}) + a \qquad [1]$$

$$\log \rho_{1000^{\circ}\text{C annealed}} = K_2\,(\text{Si/W}) + b \qquad [2]$$

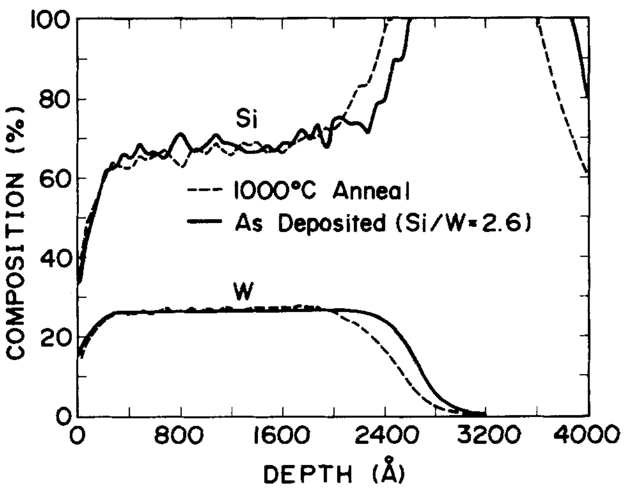

**Fig. 6.** RBS depth profiles of Si and W before and after 1000°C annealing for a Si/W ratio of 2.6.

Where $K_1$ and $K_2$ are +0.44 and +0.87, respectively; $a$ and $b$ are −4.18 and −6.17, respectively. From the values of $K_1$ and $K_2$, it is found that the composition dependence of the resistivity after 1000°C annealing is about twice as large as that of the resistivity in the as-deposited state. The speculation is as follows. The structure of the $WSi_x$ films in the as-deposited state is amorphous and their densities are low. For this reason, the resistivity of $WSi_x$ films is not sensitive to the Si/W ratio. After 1000°C annealing, $WSi_x$ crystals begin to crystallize, and the films are densified. In this case, the resistivity of the $WSi_x$ films is more sensitive to the Si/W ratio, since the amount of $WSi_x$ crystals that have low resistivity is proportional to the ratio of tungsten.

*Change in composition and segregation of excess Si by annealing.*—The composition before and after 1000°C annealing as a function of substrate temperature is shown in Fig. 5. The change in composition between the as-deposited state and after 1000°C annealing becomes larger as the substrate temperature rises and the composition becomes richer in Si. To investigate whereabouts of excess Si when the composition changes, we analyzed depth profiles of Si and W before and after the 1000°C annealing for Si/W ratios ranging from 2.6 to 3.0 by RBS. The results are shown in Fig. 6 and 7. In the film with a Si/W ratio of 2.6, there is no change in composition, and only a decrease in film thickness occurs. On the other hand, in the film with a Si/W ratio of 3.0, it has been found that a change in composition and a decrease in film thickness occur together. Also an excess Si segregation was observed in the boundary between $WSi_x$ and poly-Si. This fact is explained as follows. From Fig. 7, it is understood that for the 1000°C annealed sample, about half the volume of the whole film has a Si concentration higher than that in the as-deposited sample. This indicates that the region of higher Si concentration moves from the boundary toward the surface. This phenomenon can be explained by the decrease in the thickness of the film and the Si segregation. In this case, the region of higher Si concentration is 1.5 times as large as that of the calculated volume decrease (see Fig. 8). Consequently, Si must be segregated in the boundary region between $WSi_x$ and poly-Si.

*Decreasing of film thickness.*—The volume decrease of $WSi_x$ is given in Eq. [3] when $WSi_x$ is crystallized (11)

$$\Delta V = -\frac{(V_W + xV_{Si}) - V_{WSi_x}}{(V_W + xV_{Si})} \times 100 \qquad [3]$$

where $\Delta V$ is the volume decrease of the $WSi_x$ film, $V_W$ is the molecular volume of tungsten, $V_{Si}$ is the molecular volume of Si, and $V_{WSi_x}$ is the volume of crystallized tungsten which is represented as the sum of molecular volume of $WSi_2$ and molecular volume of excess Si or W in Eq. [4] and [5]. In the case of $x \geqq 2$

$$V_{WSi_x} = V_{WSi_2} + (x - 2)\, V_{Si} \qquad [4]$$

In the case of $x < 2$

$$V_{WSi_x} = \frac{x}{2} V_{WSi_2} + \left(1 - \frac{x}{2}\right) V_W \qquad [5]$$

The volume decrease of $WSi_x$ is shown in Fig. 8. It is obtained by substitution of Eq. [4] or [5] into [3]. A maximum is reached at Si/W = 2.

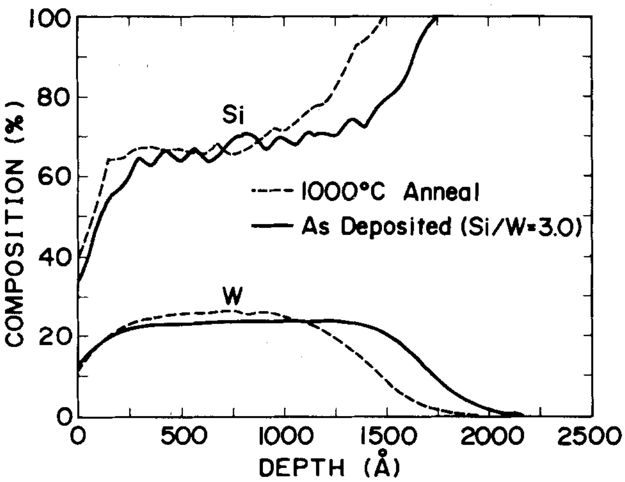

Fig. 7. RBS depth profiles of Si and W before and after 1000°C annealing for a Si/W ratio of 3.0.

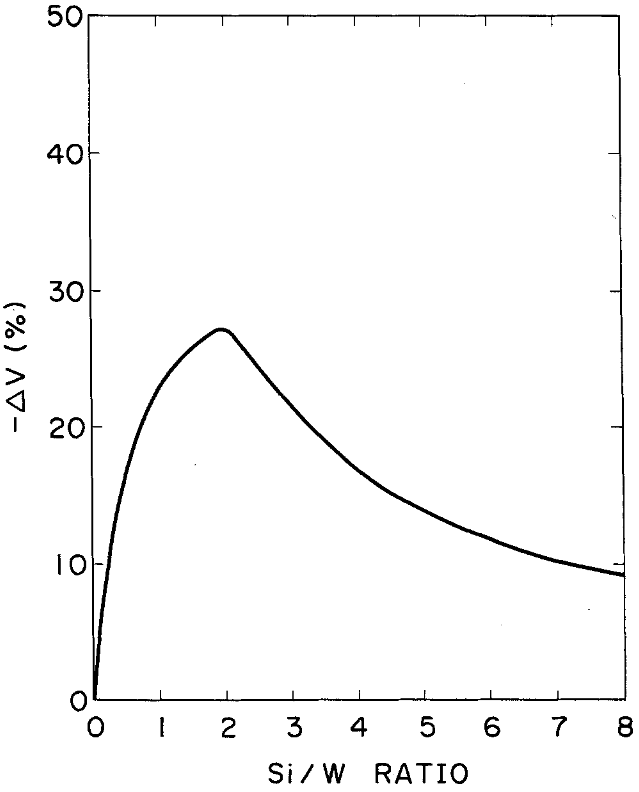

Fig. 8. Calculated volume decrease of $WSi_x$

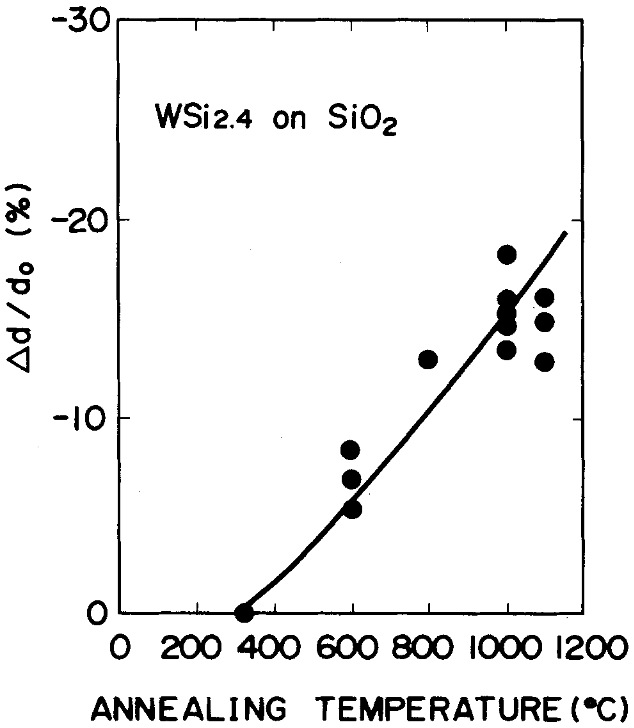

Fig. 9. Measured film thickness decrease of $WSi_{2.4}$

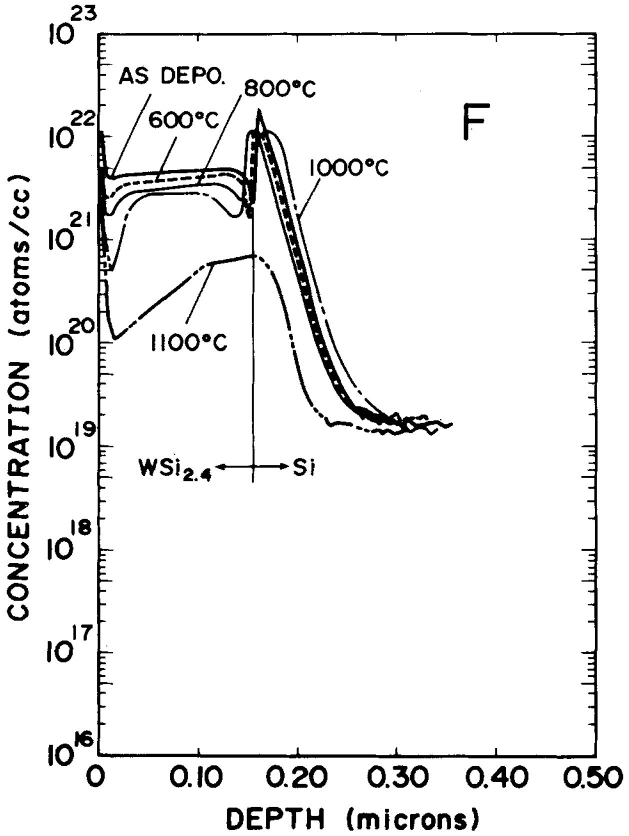

Fig. 10. Distribution of F in the $WSi_{2.4}$ film on poly-Si after annealing. Fluorine was analyzed by SIMS.

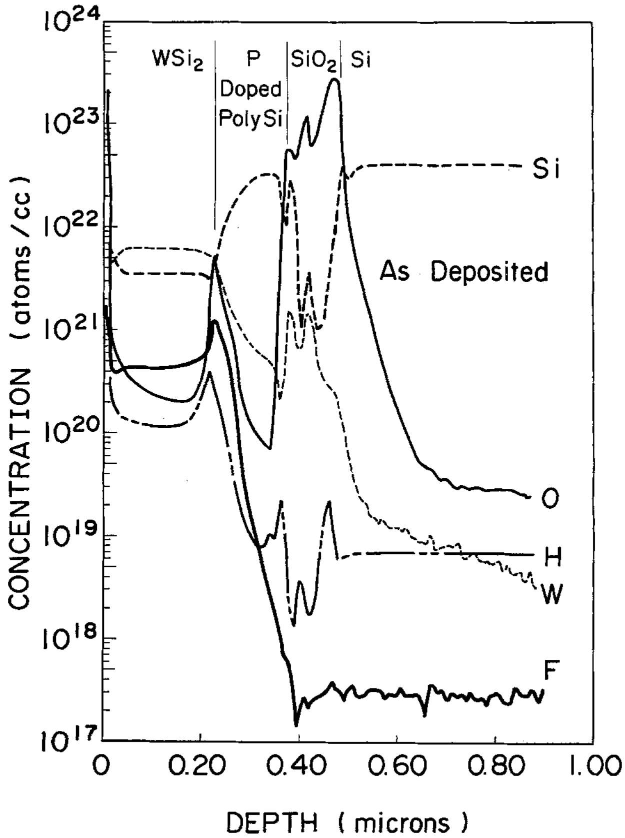

Fig. 12. Depth profiles of F and H before annealing in the $WSi_{2.4}$/poly-Si (1000Å)/$SiO_2$ (400Å) structure. Fluorine and hydrogen are analyzed by SIMS.

The measured change in film thickness is shown in Fig. 9. The values after 1000°C annealing when the film is assumed to be perfectly crystallized is smaller than the calculated value. This is because the composition after annealing remains $WSi_x$ ($x \geqq 2$) and is not separated into $WSi_2$ and Si layers. In other words, separation of the $WSi_x$ ($x \geqq 2$) to $WSi_2$ and Si is not perfect. Actually, there is a

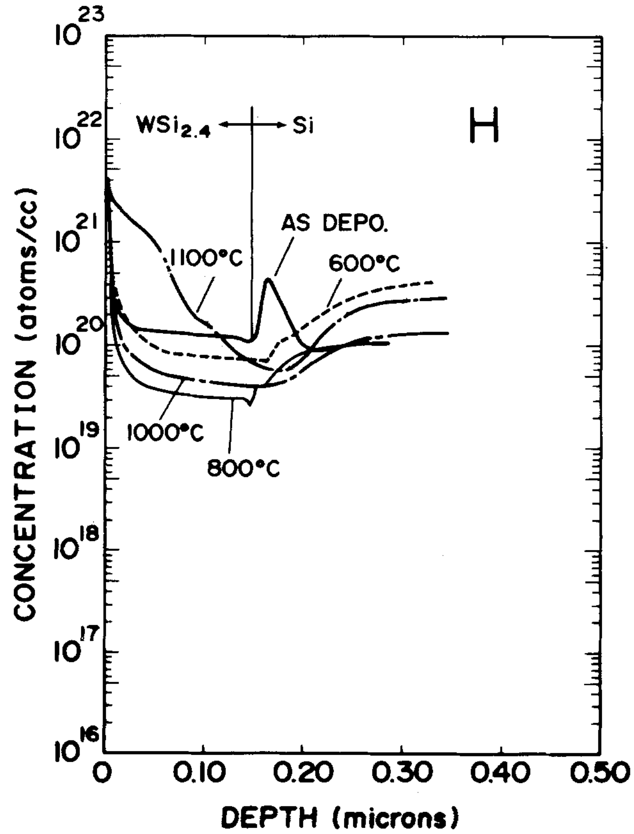

Fig. 11. Distribution of H in the $WSi_{2.4}$ film on poly-Si after annealing. Hydrogen was analyzed by SIMS.

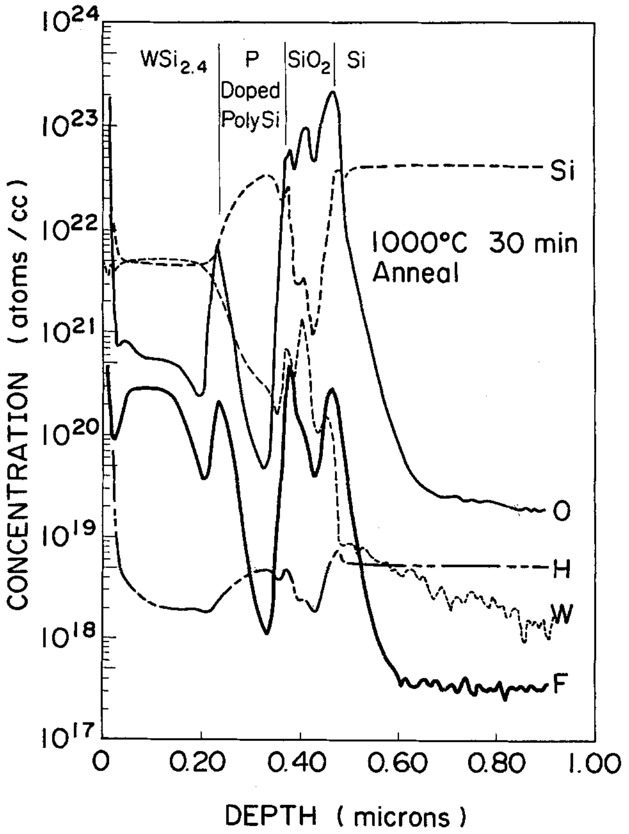

Fig. 13. Depth profiles of F and H after 1000°C annealing in the $WSi_{2.4}$/poly-Si (1000Å)/$SiO_2$ (400Å) structure. Fluorine and hydrogen are analyzed by SIMS.

lot of F and H in the film. These impurities are assumed to prevent crystallization of $WSi_x$.

The decreasing resistivity with decreasing film thickness is shown in Fig. 4. A is the resistivity in the as-deposited state, B is the resistivity after 1000°C annealing, and C is the resistivity calculated by decreasing of the film thickness only. From this figure, it can be seen that the effect on resistivity of decreasing film thickness was calculated to be less than 27.6%, whereas actually it is about 10-20%. Also, it is recognized that the effect of decreasing film thickness becomes smaller as the film becomes richer in Si.

*Distribution of F and H.*—F and H are contained to the orders of about $10^{21}$ and $10^{20}$ $cm^{-3}$, respectively, in CVD $WSi_x$ film (12). The distribution of F and H after annealing is shown in Fig. 10 and 11, respectively (12). The concentrations of F and H are gradually decreased with annealing. It is considered that the movement of these impurities from the $WSi_x$ film promotes crystallization and accelerates densification. Depth profiles of F and H, in the $WSi_{2.4}$/poly-Si (1000Å)/$SiO_2$ (400Å) structure are shown in Fig. 12 and 13. These impurities are analyzed by SIMS. It is recognized that F diffuses into $SiO_2$ by annealing. From these figures, it can be considered that there is a possibility of degradation in breakdown voltage of gate $SiO_2$ by F diffusion into gate $SiO_2$ from $WSi_x$. In this case, phosphorous concentration in poly-Si is $1 \times 10^{21}$ $cm^{-3}$ and $3 \times 10^{19}$ $cm^{-3}$ before and after 1000°C annealing, respectively.

## Summary

The change in resistivity and composition of $WSi_x$ films is studied. The following facts are observed. The resistivity of CVD $WSi_x$ films which are more than 1000Å thick reaches a maximum at an annealing temperature ranging from 500° to 600°C. Logarithmical resistivities before and after 1000°C annealing have a linear relation to the film composition. The ratio of change in resistivity between the as-deposited state and after 1000°C annealing becomes larger as the composition changes, *i.e.*, the Si/W ratio becomes smaller and reaches the stoichiometric value.

The change in composition between the as-deposited state and after 1000°C annealing becomes larger as the film become richer in Si. Excess Si, which is generated by annealing, segregates into the boundary between $WSi_x$ and poly-Si. A decrease in film thickness of about 15% after 1000°C annealing is observed for $WSi_{2.4}$ on $SiO_2$. This value is smaller than the calculated value.

Fluorine and hydrogen are contained in the films on the order of $10^{21}$-$10^{20}$ $cm^{-3}$ and $10^{20}$-$10^{19}$ $cm^{-3}$, respectively. Fluorine diffuses into the gate $SiO_2$ by annealing. From this fact, it is assumed that degradation of gate $SiO_2$ in terms of dielectric breakdown strength can occur.

## Acknowledgment

The authors would like to express their gratitude to K. Wada for his encouragement in this study.

Manuscript submitted Nov. 4, 1985; revised manuscript received March 10, 1986.

*Fujitsu Limited assisted in meeting the publication costs of this article.*

## REFERENCES

1. J. Yamada, T. Mano, J. Inoue, S. Nakajima, and T. Matsuda, *ISSCC Dig. Tech. Papers*, 104 (1984).
2. K. Itoh, R. Hori, J. Etoh, S. Asai, N. Hashimoto, K. Yagi, and H. Sunami, *ibid.*, 280 (1984).
3. F. Horiguchi, Y. Itoh, and H. Iizuka, *ibid.*, 244 (1985).
4. Y. Takemae, T. Ema, M. Nakano, F. Baba, T. Yabu, K. Miyasaka, and K. Shirai, *ibid.*, 250 (1985).
5. A. Akimoto and K. Watanabe, *Appl. Phys. Lett.*, **39**, 445 (1981).
6. Y. Ohyama, Y. Shioya, M. Maeda, and M. Takagi, *J. Vac. Soc. Jpn.*, **26**, 831 (1983).
7. D. L. Brors, J. A. Fair, K. A. Monnig, and K. C. Saraswat, *Solid-State Technol.*, **26**, 183 (1983).
8. M. Fukumoto, A. Shinohara, S. Okada, and K. Kugimiya, *IEEE Trans. Electron Devices*, **ed-31**, 1432 (1984).
9. T. Hara, S. Enomoto, and T. Jinbo, *Jpn. J. Appl. Phys.*, **23**, L455 (1984).
10. Y. Shioya and M. Maeda, *J. Appl. Phys.*, To be published.
11. S. P. Murarka, *J. Vac. Technol.*, **17**, 775 (1980).
12. Y. Shioya, T. Itoh, S. Inoue, and M. Maeda, *J. Appl. Phys.*, **58**, 4194 (1985).

---

# Optimization of Submicron Polysilicon Etching and the Effect of Organic and Inorganic Masks, and Their Aspect Ratios

**Shiesen Peng, Devereaux C. Chen, and E. D. Liu**

*Hewlett-Packard Laboratories, Palo Alto, California 94304*

## ABSTRACT

Factors that influence the etching properties of LPCVD deposited polysilicon were investigated. These included pressure, power, $CCl_4$ concentration, surface preparation, polysilicon doping, mask angle, mask material, and mask aspect ratio. Organic mask etch rate was found to depend on the type of resist (PMMA, PCMS, AZ1470), while resist preparation and mask aspect ratio were seen to influence the etch profiles. We were able to obtain vertical etch profiles using inorganic masking ($Si_3N_4$). A new phenomenon of transition from anisotropic to nonanisotropic etching was observed when the height-to-gap-width aspect ratio of the organic masks became greater than 6:1. The degree of negative undercut became more severe with increasing aspect ratio.

In VLSI processes, the ability to define submicron features becomes absolutely necessary as devices are scaled to smaller dimensions (1). This is especially critical at the gate level in MOS processes where polysilicon etching is required. For several years, workers have been investigating the polysilicon process using plasmas. Typically, they have not been able to meet all of the following key requirements simultaneously: zero undercut for linewidth preservation, good selectivity to underlying gate oxide, no residue formation in unmasked areas, and low resist erosion rate. In order to meet these requirements, we have found it necessary to investigate the physical parameters that influence the etching process. The etching process is critically dependent upon polymer formation (2), which is in turn dependent upon variables such as reactor pressure, etchant gas concentration, electrode power, etc.

There also arises a need to understand the impact of electron-beam resists on the polysilicon etching process as electron beams become increasingly employed for submicron patterning (3, 4). In this study, we have investigated the influence of several of these resists on the etching process.